UCRL-16706

University of California

Ernest O. Lawrence Radiation Laboratory

TWO-WEEK LOAN COPY

This is a Library Circulating Copy which may be borrowed for two weeks. For a personal retention copy, call Tech. Info. Division, Ext. 5545

STUDIES OF FRAGMENT ANGULAR DISTRIBUTIONS IN THE FISSION OF Bi^{209} AND U^{238} INDUCED BY ALPHA PARTICLES OF ENERGIES UP TO 115 MeV

Berkeley, California

DISCLAIMER

This document was prepared as an account of work sponsored by the United States Government. While this document is believed to contain correct information, neither the United States Government nor any agency thereof, nor the Regents of the University of California, nor any of their employees, makes any warranty, express or implied, or assumes any legal responsibility for the accuracy, completeness, or usefulness of any information, apparatus, product, or process disclosed, or represents that its use would not infringe privately owned rights. Reference herein to any specific commercial product, process, or service by its trade name, trademark, manufacturer, or otherwise, does not necessarily constitute or imply its endorsement, recommendation, or favoring by the United States Government or any agency thereof, or the Regents of the University of California. The views and opinions of authors expressed herein do not necessarily state or reflect those of the United States Government or any agency thereof or the Regents of the University of California.

Submitted to Physical Review

UCRL-16706

UNIVERSITY OF CALIFORNIA

Lawrence Radiation Laboratory
Berkeley, California

AEC Contract No. W-7405-eng-48

STUDIES OF FRAGMENT ANGULAR DISTRIBUTIONS IN THE FISSION OF Bi^{209} AND U^{238} INDUCED BY ALPHA PARTICLES OF ENERGIES UP TO 115 MEV

S. S. Kapoor, H. Baba and S. G. Thompson

February 14, 1966

STUDIES OF FRAGMENT ANGULAR DISTRIBUTIONS IN THE FISSION OF Bi^{209} AND U^{238} INDUCED BY ALPHA PARTICLES OF ENERGIES UP TO 115 MEV*

S. S. Kapoor,† H. Baba‡ and S. G. Thompson

Lawrence Radiation Laboratory
University of California
Berkeley, California

February 14, 1966

ABSTRACT

Using semiconductor detectors, the fragment angular distributions have been measured in the cases of fission of Bi^{209} and U^{238} induced by alpha particles of various energies ranging from 23 MeV to 115 MeV obtained from the Berkeley 88-inch variable-energy cyclotron. The center of mass angular distributions were analyzed by a least-squares fitting code to obtain the value of K_o^2 corresponding to the saddle point excitation energy Ex^s for each bombarding energy. The transmission coefficients T_ℓ and the mean square of the orbital angular momentum $\langle \ell^2 \rangle$ of the fissioning nucleus required for deducing K_o^2 were determined from optical model calculations. For both the cases of compound nuclei of At^{213} and Pu^{242}, it is found that the values of K_o^2 increase more rapidly with Ex^s than expected on the basis of the Fermi gas model, irrespective of the assumptions made about the multiple chance fissions. The fission cross sections of U^{238} for alpha particle energies up to 110 MeV, also measured in this work, enabled us to check the accuracy of the optical model calculations. The presence of direct interactions and their effects on the deduced values of K_o^2 were also investigated in detail in the case of the target nucleus U^{238}. Using the standard expression for Γ_n/Γ_f, the first chance values of K_o^2 have been obtained and further corrected for the estimated direct interaction effects, in the case of the target nucleus U^{238}. Even after allowance is made for the direct interaction effects, the energy dependence of K_o^2 appears to be significantly different from that expected on the basis of the simple Fermi gas

model. These results can be explained within the framework of the Fermi gas model if it is assumed that $J_{eff}/a_f^{\frac{1}{2}}$ increases significantly with the bombarding energy. It appears likely that these results suggest a rapid increase in the effective moment of inertia J_{eff} with the angular momentum as can be expected on the basis of the observed steep variation in the saddle shapes with Z^2/A.

I. INTRODUCTION

In the last few years, several measurements on the angular distribution of the fragments in the fission of a number of nuclei induced by a variety of projectiles have been reported.[1] The interpretation of these angular distributions and further developments in this field are primarily based on a model proposed by A. Bohr.[2] The underlying idea of the model is that the stretched fissioning nucleus in passing over the saddle point exhibits quantum states similar to those observed in the permanently deformed nuclei, except that the states of the saddle point nucleus are expected to be quasistationary since the nucleus spends a very small time at the saddle point. The orientation of the fissioning nucleus at the saddle point, then, depends on the available quantum states characterized by $\vec{I}$, $\vec{M}$ and $\vec{K}$, where $\vec{I}$ is the total angular momentum of the nucleus, $\vec{M}$ is the projection of $\vec{I}$ on a space fixed axis (taken as the incident beam direction) and $\vec{K}$ is the projection of $\vec{I}$ on the symmetry axis of the fissioning nucleus. By assuming that $\vec{K}$ is conserved from saddle point to scission point, the expected angular distribution of the fission fragments can be calculated by averaging over the distributions of the $\vec{I}$, $\vec{M}$ and $\vec{K}$ states available at the saddle point. In the case of medium energy fission, where the angular momentum deposited by the projectile on the compound nucleus is much larger than any possible spin of the target nucleus or the projectile, a simplification emerges from the fact that $\vec{M} \approx 0$. The distribution in the I-states can be obtained from an optical model calculation of the particle transmission coefficients as a function of $\vec{I}$. With such considerations Halpern and Strutinski[3] and Griffin[4] have extended the Bohr model to the case of medium energy fission by further applying statistical considerations at the saddle point to determine the distribution in the available K-states. The fission fragment anisotropy is then found to depend on the parameter $p = \langle I^2 \rangle / 2K_o^2$, where K_o is the standard deviation of the assumed Gaussian distribution of the K states. Here it is assumed that the K-distribution is that of the internal states of the nucleus corresponding to the saddle point excitation energy; therefore, on the basis of the statistical theory K_o^2 is connected with the effective moment of inertia J_{eff} and the nuclear temperature T of the saddle point nucleus by the relation

$$K_o^{\ 2} = J_{eff} \cdot T/\hbar^2 \quad . \tag{1}$$

The effective moment of inertia J_{eff} is defined as

$$J_{eff} = J_{\perp} J_{\parallel}/(J_{\perp} - J_{\parallel}) \quad , \tag{2}$$

where $J_{\parallel}$ and $J_{\perp}$ are the moments of inertia about axes parallel to and perpendicular to the fission axis, respectively. On the basis of the Fermi gas model, it is therefore expected that

$$K_o^{\ 2} = \frac{J_{eff}}{\hbar^2} \cdot \frac{(Ex^s)^{\frac{1}{2}}}{a_f^{\frac{1}{2}}} \quad , \tag{3}$$

where Ex^s is the excitation energy and a_f is the nuclear level density parameter both corresponding to the saddle point configuration of the nucleus. The values of $K_o^{\ 2}$ (and hence J_{eff}) can, therefore, be extracted from the measurements on the fragment angular distributions and thereby information on the saddle point shapes can be obtained if a rigid body value is assumed for J_{eff}. These studies have been recently made by Reising et. al.[5] where the values of J_{eff} are derived from measurements of the fragment anisotropies in the 42.8 MeV alpha induced fission of a variety of nuclei.

The analysis of the angular distributions is relatively simple if the observed fissions correspond primarily to first chance fissions and, therefore, to a single value of Ex^s. But at those energies where multiple chance fissions contribute significantly to the observed distributions, the analysis of the angular distributions requires a knowledge about the relative number of nuclei undergoing fission at different excitation energies. In other words, for such cases it is necessary to know how Γ_n/Γ_f varies with the excitation energy and mass number. Conversely, one might expect to obtain some information concerning the number of neutrons emitted before fission from the measurements of fragment anisotropies provided that other complicating processes do not set in at these higher energies, and the theoretical framework remains justified throughout the energy range. At the higher bombarding energies of alpha particles, say from 40 MeV to 110 MeV, where multiple chance fissions are

expected both in the medium and heavy weight nuclei, to our knowledge there are at present almost no data on the behavior of fragment anisotropies with the bombarding energies. Consequently very little is known about the new processes involved and the validity of the proposed theoretical framework in this energy region. We have carried out detailed measurements of the fragment angular distributions in the alpha induced fission of Bi^{209} and U^{238}, at various alpha particle bombarding energies ranging from about 30 MeV to 115 MeV. On analyzing the data within the standard theoretical framework it is found that K_o^2 varies significantly more rapidly with the excitation energy than expected on the basis of a Fermi gas dependence, irrespective of the assumptions made about multiple chance fissions. In the case of the bombardment of U^{238}, it has been possible to experimentally check the optical model calculations of $\langle \ell^2 \rangle$ and to correct for the direct interaction effects and the multichance fissions, and, therefore to quantitatively evaluate the deviations of first chance K_o^2 with theory. Though these results may be taken to point out a rapid variation of J_{eff} with angular momentum, questions may also be raised regarding the energy dependence of K_o^2.

II. EXPERIMENTAL

Beams of alpha particles of different energies up to 115 MeV were obtained from the 88-inch variable-energy cyclotron[6] at Berkeley. The emergent beam passed through a quadrupole focussing magnet and was then deflected into the experimental area by a switching magnet where the beam was further focussed by a second quadrupole magnet to obtain a sharp beam spot at the center of the target position in the experimental vacuum chamber. The final focussing adjustments were made by placing a gridded quartz disc at the otherwise target position, and by observing the beam spot through the light emitted from the irradiated area of the quartz. A steel cylinder of about 9.5-cm length having a collimator in the center of the side facing the beam was placed in the beam pipe. This collimator restricted the beam area to a circle of 0.3-cm diameter. The beam then further passed through three graphite collimators spaced 7.3 cm apart and each provided with holes of 0.4-cm diameter to ensure that its edges would not be struck by the beam. The distance of the last collimator from the target position was about 14 cm.

The vacuum chamber used is similar to the one described elsewhere.[7] After passing through the target, the beam was collected in a Faraday cup connected to an integrator, which measured the integrated beam current. The bismuth targets were prepared by the standard volatilization process, using bismuth of the highest available purity, and self-supporting foils of thickness 239 $\mu g/cm^2$ were used in the measurements. The uranium targets, made by vacuum evaporation of $U^{238}O_2$ onto $\sim$ 70 $\mu g/cm^2$ carbon backings, were obtained from the Los Alamos Scientific Laboratory. The U^{238} target was made of depleted U^{238} with a contamination of 0.03% U^{235}. The thickness of the uranium target was 110 $\mu g/cm^2$. The target films were mounted on stainless steel rings of $\frac{1}{2}$-in. inner diameter, and measurements were made with the targets mounted at the standard angle of 45° with respect to the beam direction.

The fragment detectors were phosphorous diffused semiconductor detectors of 400 ohm-cm p-type silicon and of 1 cm $\times$ 1 cm square size, which were operated at reverse bias of 40 volts. The chamber had two movable arms each of which could be set at any angle from 0° to 180° with respect to the beam direction in the two halves of the chamber. Three fragment detectors D_1, D_2 and D_3 were mounted on one of the arms

with an angular separation of 20°, and such that each of the detectors was at a distance of 12.7 cm from the target center. The fourth detector D_4 was mounted at exactly the same distance on the other arm in the other half of the chamber. With this geometry the maximum angle of divergence from the mean detection angle is about $\pm 2^{\circ}$. The pulses from each detector preamplifier were fed to a standard transistorized amplifier followed by a discriminator to cut off any alpha pulses caused by the scattering of the beam. The amplifier outputs gated by the respective discriminators were simultaneously recorded on a 400 channel analyzer used as four analyzers of 100 channels each. The adjustments in the discriminator level of each of the systems were made to cut off any low energy tail in the recorded spectrum. The low energy ends of the recorded spectra were also finally examined and the counts recorded in each of the scalers were corrected for any residual low energy tail in the corresponding spectrum. The tail correction in general was less than about one percent.

The angular distributions were measured by changing the angle of the arm carrying the three detectors, while keeping the detector D_4 at a fixed angle of 90° in the other half of the chamber to serve as a monitor. During some of the runs, where there was also interest in the measurement of total fission cross sections, the integrated beam current was used as a monitor. With the present collimating device and the focussing adjustments, the beam spot on the target could be off the center by not more than 1 to 1.5 mm. Even this non-centering of the beam could cause a change in the solid angles of detection at 170° and 90° by about 2.5% in opposite directions, changing the ratio of solid angles by about 5%. However, by counting the fragments at 90° on both sides of the target by means of detectors D_2 and D_4, it was possible to correct experimentally for any non-centering of the beam position on the target. Using a Cf^{252} fission source, it was first insured that the solid angles subtended by the two detectors are the same within 1%. Any small deviation of the beam position from the target center which could appreciably change the solid angle of detection at various angles was obtained from the differences in the counts of D_2 and D_4 detectors, and the angular distributions were corrected for this effect. Further, any small differences in the detection geometries of the three

detectors (D_1, D_2 and D_3) were obtained from the data in which the fragments were counted at the same angle but with different detectors, and these were also taken into account in obtaining the angular distributions from the recorded data. The angular distributions for most of the cases were measured at angular intervals of 5° from 170° to 90° (in the backward direction), and at a few angles in the forward direction. In all the runs, the angle of emission of the detected fragments with the plane of the foil was kept greater than 45°. Hence, in those cases where the fragments were detected in the forward directions, the foil was rotated by 90°.

III. EXPERIMENTAL RESULTS

The measured angular distributions were transformed to the center of mass system with the assumption of full momentum transfer of the alpha particles to the compound nucleus. In fact, the measurements on the fragment-fragment angular correlations, as described later, show that in the case of the less fissile nucleus Bi^{209} practically all the fission events correspond to the case of full momentum transfer even at the extreme bombarding energy of 110 MeV. Even in the case of U^{238}, it is found that the fraction of fission events corresponding to incomplete momentum transfer at 110 MeV bombarding energy is too small to significantly affect the results of transformations. The average values of the kinetic energy of the fragments, equal to 74 MeV for the compound nucleus At^{213} and 86 MeV for the compound nucleus Pu^{242}, were used in the transformations. For a typical case of alpha particle energy of 100 MeV, the measured angular distributions plotted in the center of mass system are shown in Fig. 1 for the above two targets. It can be seen that the points measured in the backward and the forward angles describe nearly the same curve, providing, in a direct way, a justification for the assumptions used in the transformation. The least-squares fits to the angular distributions were made with Legendre Polynomials, terminating the number of terms of the Legendre Polynomial at a value such that the X^2 changes by less than 2% in going to the next term. The observed anisotropies $N(171^\circ)/N(90^\circ)$ and the coefficients resulting from the least squares fits for the various

alpha bombarding energies are summarized in Table I for the two targets. It can be seen that even at the highest bombarding energies, the higher terms are not statistically significant. For the typical case shown in Fig. 1, the Legendre polynomial least-squares fit to the data is also shown.

The statistical error on the anisotropy in each measurement was about one percent except for the first two low energy points in the case of fission of Bi^{209}. However, even after correcting for the beam position on the target, the data were found to be reproducible only within about 2 to 3 percent, possibly due to the presence of certain other unknown systematic errors. These larger errors are therefore assigned to the values of the measured anisotropies given in Table I. Figure 2 shows a plot of the measured anisotropies for the case of alpha induced fission of U^{238}. For the sake of comparison and completeness, the results obtained by Vandenbosch, et. al.[8] and by Leachman and Blumberg[9] for the alpha particle bombarding energies of less than 45 MeV are also shown in the figure, and these results are found to be in good agreement with the present measurements. Qualitatively, the increase in the anisotropy with the bombarding energy in a step-like fashion in the energy range of 20 MeV to 60 MeV can be understood on the basis of the increasing angular momentum and the onset of (α,xnf) processes. But it appears to be an unforeseen result that the anisotropy is nearly constant or slightly decreases for bombarding energies higher than 60 MeV. The same trend can be seen in the case of fission of Bi^{209}, where the anisotropy is constant for bombarding energies higher than about 70 MeV. These results are discussed later in a quantitative way.

IV. ANALYSIS OF RESULTS AND DISCUSSION

A. Comparison With Theory

The observed angular distribution of the fragments in the center of mass system have been analyzed to deduce the values of K_o^2 for various alpha particle bombarding energies on the basis of the model proposed by Halpern and Strutinski.[3] According to the theory, the differential cross section for fission at the center of mass angle θ, relative to the value at 90° is given by

$$\frac{W(\theta)}{W(90^o)} = \frac{\int_0^{\ell_m^2} \ell \exp\left(\frac{-\ell^2 \sin^2\theta}{4K_o^2}\right) J_o\left(\frac{i\ell^2 \sin^2\theta}{4K_o^2}\right) d\ell^2}{\int_0^{\ell_m^2} \ell \exp\left(\frac{-\ell^2}{4K_o^2}\right) J_o\left(\frac{i\ell^2}{4K_o^2}\right) d\ell^2} , \qquad (4)$$

where J_o is the zero order Bessel function, and ℓ_m is the maximum angular momentum brought in by the incident particle. The above expression assumes that the target and projectile spins are zero, and the particle deposits in the nucleus all values of the angular momentum up to the maximum value ℓ_m with a uniform probability per unit ℓ^2. Further, a possible weak dependence of fissionability on the angular momentum ℓ has been neglected here. In the present experiments, we are actually dealing with a zero spin target in the case of U^{238}, and calculations show that even for the case of Bi^{209} (spin 9/2) the effect of the target spin on the anisotropy is negligible in the present cases where large angular momenta are brought in by the incident projectile. The total angular momentum of the nucleus is therefore taken equal to the orbital angular momentum ℓ of the incident projectile. The actual distribution in ℓ obtained from optical model calculations of the particle transmission coefficients T_ℓ as a function of ℓ shows that the probability distribution for the momentum deposited is, in general, rounded at the top end rather than being uniform in ℓ^2 throughout, as assumed in Eq. (4). But it is known that the anisotropy calculated from the above expression corresponds very nearly to the actual case, if the appropriate value of ℓ_m^2 is taken as $\ell_m^2 = 2 \langle\ell^2\rangle$, where $\langle\ell^2\rangle$ is the average value of the square of the angular momentum. As shown later, the computations

carried out in the present work also confirm this. According to Eq. (4) the anisotropy depends on the parameter $p = \langle \ell^2 \rangle / 2K_o^2$, which can therefore be obtained by a least-squares fit of the experimental angular distributions to Eq. (4). The value of $\langle \ell^2 \rangle$ for the compound nuclei formed can be obtained from the relation

$$\langle \ell^2 \rangle = \frac{\sum \ell^2 \, (2\ell + 1) \, T_\ell}{\sum (2\ell + 1) \, T_\ell} \quad . \tag{5}$$

Without introducing the simplifying assumptions regarding the shape of the ℓ-distribution, the following exact expression for the differential cross section can be obtained by summing the cross section for each state ℓ:

$$\frac{W(\theta)}{W(90^\circ)} = \frac{\sum_\ell (2\ell + 1) T_\ell \, \ell \exp\left(\frac{-\ell^2 \sin^2\theta}{4K_o^2}\right) J_o\left(\frac{i\ell^2 \sin^2\theta}{4K_o^2}\right)}{\sum_\ell (2\ell + 1) T_\ell \, \ell \exp\left(\frac{-\ell^2}{4K_o^2}\right) J_o\left(\frac{i\ell^2}{4K_o^2}\right)} \quad . \tag{6}$$

The observed center of mass angular distributions were fitted to both Eqs. (4) and (6) with a least-squares fitting code using an IBM 7044 computer to obtain in each case the value of K_o^2. The values of T_ℓ and $\langle \ell^2 \rangle$ were computed from an optical model code as described in Section C. The values of K_o^2 resulting from the least-squares fitting of the data are summarized in Tables II and III for the cases of fission of Bi^{209} and U^{238}, respectively. It can be seen from Tables II and III that there is no significant difference in the values of K_o^2 obtained from fitting to Eqs. (4) and (6), which shows that the simplifying assumptions introduced in deriving Eq. (4) do not introduce any significant error. For simplified presentation we have therefore discussed the results mostly in terms of the parameter $\langle \ell^2 \rangle / 2K_o^2$, denoted by p.

The binding energies of the alpha particles to the respective target nuclei, which were used to calculate the excitation energies Ex, were taken from the compilations of Everling et. al.[10] The excitation energy Ex^s for the saddle point configuration was calculated from the

relationship[11],

$$Ex^s = Ex - E_{PP} - \Delta - E_R^o \quad , \tag{7}$$

where E_R^o is the rotational energy of the spherical compound nucleus, E_{PP} is the energy of a rotating saddle point configuration (referred to as the Pik-Pichak shape) above that of the rotating sphere and Δ is the shell correction energy.

In the case of Bi^{209}, the values of E_{PP} for different rotational energies were obtained from the calculations[11,12] on the rotating liquid drop, and a value[13] of Δ equal to 3.6 MeV was used. In effect, the calculated values of $(E_{PP} + \Delta)$ vary from 16.2 MeV for the case of zero angular momentum to 13.6 MeV for $\ell \sim 30$ units (average value of the angular momentum in the bombardment with 115 MeV alphas). In the case of U^{238}, the values of $(E_{PP} + \Delta)$ are denoted by E_B in Table III. In this case a value of 4.9 MeV was used for the ℓ=0 case; this decreased with the angular momentum to a value of 3.2 MeV for $\ell \sim 31$ units (average angular momentum produced in the bombardment with 115 MeV alphas). The values of Ex^s calculated in this way correspond to the case of first chance fission. In the present range of bombarding energies, in both the cases of fission of Bi^{209} and U^{238}, it is expected that the observed fissions correspond to several values of Ex^s due to fissions taking place after the emission of zero, one or more neutrons or other particles, and therefore the deduced K_o^2 represent some average values over the various chance fissions. These values of K_o^2 are plotted against Ex^s (calculated for the first chance fission) in Figs. 3 and 4 for the cases of fission of Bi^{209} and U^{238}, respectively. The solid line in Fig. 3 represents the values of K_o^2 given by the Fermi gas model (Eq. 3). This was obtained by normalizing to the value of K_o^2 deduced from the measurements with the 40 MeV bombarding energy of alpha particles where essentially all the observed fissions take place with a single value of Ex^s corresponding to first chance fission. The shaded area around the solid line corresponds to the uncertainty in the normalization constant based on the estimated uncertainty in the measured value of K_o^2 at the normalizing point. For the sake of comparison with the present results, the values of K_o^2 obtained by Chaudhry, et. al.[14] in the range of energy[15] Ex^s between about 4 to 16 MeV are also shown in Fig. 3. It

can be seen that the energy dependence of K_o^2 as calculated from Eq. (3) after normalizing to the present results with 40 MeV alpha particles gives a good fit to the values of K_o^2 deduced in their measurements.

It is apparent from Fig. 3 that although the values of K_o^2 deduced in the small energy range of Ex^s up to about 16 MeV can be fitted to the dependence given by the Fermi gas model, the experimental values of K_o^2 become significantly larger than theory with increasing excitation energy even if it is assumed that the observed fissions correspond to first chance fissions. If multichance fissions are taken into account, one instead expects the values of K_o^2 to be lower than those given by the shaded region, and consequently the deviations with the theory are, in fact, more serious than apparent in the figure. Figure 4 shows the deduced values of K_o^2 for the case of fission of Pu^{242}. The values of K_o^2 deduced at two different low excitation energies by Simmons, et. al.[16] and Viola, et. al.[17] are also shown in this figure. The dotted curve has been drawn through the experimental points in a smooth fashion to represent the observed variation of K_o^2 with Ex^s. A more rapid increase in the values of K_o^2 with Ex^s than given by the square root dependence expected on the Fermi gas model is also evident in the case of fission of Pu^{242}, as can be seen in Fig. 4. The plot of $K_o^2/(Ex^s)^{\frac{1}{2}}$ versus Ex^s shown in Fig. 5 brings out more clearly the observed deviation from the theory. On the basis of the statistical theory, it is expected that $K_o^2/(Ex^s)^{\frac{1}{2}}$ should be constant at higher energies where the pairing effects[18] expected at low energies have disappeared. However, the present results show that $K_o^2/(Ex^s)^{\frac{1}{2}}$ is increasing with Ex^s even for values of Ex^s up to 100 MeV.

From the above simplified discussion, it appears that in both the cases of fission of At^{213} and Pu^{242}, the values of K_o^2 increase more rapidly with the excitation energy than expected, irrespective of any assumptions about multichance fissions. However, to make quantitative comparison with the theory it is necessary to evaluate the values of first chance K_o^2, and also to take into account the ℓ-dependence of the fissionability. Moreover, since the deduced values of K_o^2 depend crucially on the calculated values of $\langle \ell^2 \rangle$, it is desirable to check experimentally the results of optical model calculations. Finally, it

is also necessary to investigate the effect of possible direct interactions at high bombarding energies on the deduced values of K_o^2. As discussed in later sections, for the case of bombardment of U^{238} it has been possible to check experimentally the results of optical model calculations, and to obtain information on the values of first chance K_o^2 corrected for the effect of a small measured fraction of direct interaction events to enable a quantitative comparison with the expected energy dependence of K_o^2.

B. First Chance K_o^2

The effect of neutron emission on the magnitude and direction of $\vec{I}$ is, in general, not expected to be significant even at the extreme alpha particle energies of 110 MeV. For the case of U^{238} at this bombarding energy the average initial angular momentum $\langle \ell \rangle$ is about 27, the average angular momentum $\langle \ell_n \rangle$ carried by the neutrons is about 2.8 and the value of the parameter $J_o \cdot T/\hbar^2$ $(=\sigma^2)$ is about 250. The ratio $\langle \ell \rangle \langle \ell_n \rangle / \sigma^2$ is, therefore, significantly less than unity and, therefore, the emitted neutrons are expected to be weakly coupled to the initial angular momentum, resulting in a nearly isotropic addition of the neutron angular momentum vector to the initial spin. As suggested by Halpern and Strutinski,[3] the small effect of the disorientation produced in $\vec{\ell}$ may as a result get cancelled with a likely increase in the value of ℓ. It is therefore reasonable to assume the same initial value of $\langle \ell^2 \rangle$ for all the fissioning species. On the other hand, the values of K_o^2 are expected to change significantly as a result of particle emission. The extraction of first chance K_o^2 from the measured angular distributions and also the determination of K_o^2 using effective $\langle \ell^2 \rangle$ which takes into account the ℓ-dependence of the fissionability, require a knowledge about the values of Γ_n/Γ_f as a function of excitation energy, angular momentum and mass number. In the case of At^{213}, these calculations on Γ_n/Γ_f depend rather sensitively on the input level density parameters a_n and a_f. But at present, apart from the uncertainties in the values of a_n and a_f, very little is known about the possible energy dependence of a_n for this near magic nucleus At^{213}. Moreover, as pointed out by Vandenbosch,[19] for the case of At^{213}, which has a large

negative alpha binding energy, a significant evaporation of alpha particles in competition with neutrons can be expected at high excitation energies. The calculations on particle competition using optical model penetrabilities and including angular momentum effects show that at the excitation energy of 110 MeV, Γ_α/Γ_n may be of the order of unity. Because of the ambiguities in the values of a_n and a_f, and complexities introduced by possible alpha particle competition, it is difficult to exactly evaluate the values of first chance K_o^2. However, to illustrate that the values of first chance K_o^2 are expected to be higher than the observed average values, the calculated values of K_o^2 for various nuclei formed as a result of neutron emission from the initial compound nucleus At^{213} are shown in Table III for the typical case of initial excitation energy corresponding to the bombardment with 110 MeV alpha particles. In these calculations we have taken into account the fact that as a result of neutron emission, although T decreases, the value of J_{eff} increases due to the increase in the value of Z^2/A. The dependence of J_{eff} on Z^2/A was taken as deduced by Reising, et. al.[5] from the measurements on fragment anisotropies. It can be seen that the net effect is that the values of K_o^2 are decreased for the nuclei undergoing fission after the emission of neutrons. Further, in the case of emission of alpha particles or any other charged particles, the values of K_o^2 of the residual fissioning nuclei are also expected to be lower because of the decrease in both the J_{eff} and T. It can therefore be concluded that whatever be the weighting factors of the various nuclei, the values of first chance K_o^2 should be significantly larger than the observed average values of K_o^2, thereby further increasing the deviations from the shaded curve (Fig. 3) based on Fermi gas theory.

In the case of fission of Pu^{242} the calculations show that neutron emission and fission are expected to be the only significant competing processes, and, therefore, it is simpler to calculate the effect of ℓ-dependence of fissionability on the deduced values of K_o^2, and to estimate the values of first chance K_o^2. The ℓ-dependence of fissionability arises from the differences in the moments of inertia of two configurations in the competing processes of neutron emission and approach to fission barrier. In the statistical picture the resulting decrease of the barrier height with the angular momentum (as seen in Table III) increases the relative probability of fission with respect

to particle emission for larger ℓ values. We have taken into account this dependence in a simplified manner by multiplying the deduced values of K_o^2 by a factor $\langle\ell^2\rangle_e/\langle\ell^2\rangle$, where $\langle\ell^2\rangle_e$ and $\langle\ell^2\rangle$ are the average values of the square of the angular momentum relevant for the compound nuclei undergoing fission and for the compound nuclei formed, respectively. The $\langle\ell^2\rangle_e$ is obtained from the relation

$$\langle\ell^2\rangle_e = \frac{\sum \ell^2(2\ell + 1)\ T_\ell\ P_f(A,Ex,\ell)}{\sum(2\ell + 1)\ T_\ell\ P_f(A,Ex,\ell)} \quad . \tag{8}$$

Here $P_f(A,Ex,\ell)$ is the probability that the nucleus with mass A, excitation energy Ex and angular momentum ℓ undergoes fission, and is given by

$$P_f = \Gamma_f/(\Gamma_f + \Gamma_n) \quad . \tag{9}$$

A computer program for the IBM 7094 was set up to correct the values of K_o^2 for the ℓ-dependence of fissionability, and to calculate the fraction of nuclei undergoing fission at different stages and thereby to deduce the value K_{o1}^2 of first chance K_o^2. The standard expression[20] for Γ_n/Γ_f with $a_n = a_f = A/\beta$ was used in these computations. For the sake of simplicity, it was assumed that the emitted neutrons carry a constant kinetic energy equal to 2T instead of a more realistic Maxwellian distribution. This simplifying assumption is not expected to introduce any significant error in the present case, since Γ_n/Γ_f changes slowly with the excitation energy throughout most of the energy range. These calculations gave the values of $\langle\ell^2\rangle_e$ appropriate for different nuclei formed after neutron emission, and, therefore, an average value of $\langle\ell^2\rangle_e$ weighted by their relative population was used. The following expression was used for calculating the first chance K_o^2:

$$\left\{(K_o^2)\ \frac{\langle\ell^2\rangle_e}{\langle\ell^2\rangle}\right\}^{-1} = \frac{\sum_{i=1} xF_i\{[J_1 + (i-1)c]\ T_i\}^{-1}}{\sum_{i=1} xF_i} \quad , \tag{10}$$

where first chance K_o^2 is then given by

$$K_{o1}^{2} = J_1 T_1 \quad . \tag{11}$$

Here xF_i are the number of nuclei of mass (A-i+1) undergoing fission at saddle point temperature T_i. The change in the effective moment of inertia J_1 ($\equiv J_{eff}/\hbar^2$) due to the change in Z^2/A resulting from neutron emission is taken into account by the factor c which was taken from the work of Reising et. al.[5] The above expression for estimating K_{o1}^{2} assumes that the observed anisotropy is equal to the weighted average of the anisotropies for fissions taking place at different stages during neutron emission. The results of numerical calculations show that there is no significant difference in the results of this simplified procedure and that of the rigorous procedure in which the normalized angular distributions are averaged to obtain the resulting angular distributions. The last six columns of Table III show the results of these calculations for values of β = 8, 15 and 23. It is apparent that for this highly fissionable nucleus of Pu^{242}, the calculated values of $\langle \ell^2 \rangle_e$ and the extracted values of first chance fission K_o^2 are not very sensitive to the assumptions regarding the level density parameters characterized by β. Moreover, the extracted values of K_{o1}^{2} are not significantly increased as compared to the average values of K_o^2 primarily due to the predominance of first chance fissions. Since in any case K_{o1}^{2} should at least be equal to K_o^2, the uncertainties in the assumption that a_n and a_f are equal, is not expected to significantly change the extracted values of K_{o1}^{2}. A plot of K_{o1}^{2} versus Ex^s is shown in Fig. 6, where the vertical open bars enclose the values of K_{o1}^{2} obtained under different assumptions about β. It can be seen that the extracted values of K_{o1}^{2} clearly show the deviation from the expected square root dependence on Ex^s. In the next two sections the optical model calculations and the direct interaction effects are examined with a view to determine any likely contribution to the observed deviations from these factors.

C. Optical Model Calculations

The values of T_ℓ and thereby $\langle \ell^2 \rangle$ were calculated for each alpha particle energy and each target nucleus with an optical model code[21] using the Woods-Saxon parameters given by Huizenga and Igo.[22] Figure 7 shows the calculated values of $\langle \ell^2 \rangle$ along with the list of the optical model parameters used in these calculations. The calculated reaction cross section σ_R can be expressed to a good degree of accuracy by the following relationship:

$$\sigma_R = 2\pi \lambda\!\!\!^{-2} \langle \ell^2 \rangle \quad . \tag{12}$$

The accuracy of the calculated $\langle \ell^2 \rangle$ can, therefore, be inferred from a comparison of the calculated σ_R with the experimental values. The measured reaction cross sections of U^{233} and U^{238} with 18-43 MeV alpha particles have been found[23] to be in good agreement with the total reaction cross section calculated with an optical model using the above parameters. In the present calculations, it has been assumed that the same parameters can also be used for alpha particles of energies up to 115 MeV. Even though the optical model parameters are expected to depend on the bombarding energy, the use of the same parameters can be justified from the fact that the calculated σ_R shows a very weak dependence on the potentials used, especially for higher bombarding energies. However, since the values of K_o^2 deduced from the experiment depend crucially on the calculated values of $\langle \ell^2 \rangle$, it is necessary to experimentally ascertain the accuracy of the present calculations of $\langle \ell^2 \rangle$. For this reason we have measured[24] the total fission cross sections for bombardment of U^{238} by alpha particles of energies up to 110 MeV. The fission cross sections measured in the present work for alpha particle energies between 40 MeV-110 MeV are shown in Fig. 8a along with the data obtained by Viola and Sikkeland[25] for alpha particles of energies up to 41.6 MeV.

The ratio σ_f/σ_R^c of the measured fission cross sections to the reaction cross sections calculated with the optical model for various alpha particle bombarding energies are shown in Fig. 8b. Since the residual nuclei formed in this bombardment have low fission barriers (~ 5 MeV) and high excitation energies, the probability of the nucleus to fission at some stage of the competition between neutron emission and fission is very large. The observed ratio σ_f/σ_R^c of about 0.9 in the

region of alpha particle energies of 40 MeV is consistent with the measurements of Wing, et. al.[26] which shows that in this energy range the spallation cross section is about 9% of the total reaction cross section. For alpha particle energies larger than 70 MeV, the measured fission cross sections are less than the calculated reaction cross sections by about (10 ± 5)%. A fraction of this order can again be expected for the spallation cross sections at these higher energies, if the fraction of interactions corresponding to the incomplete momentum transfer have increased as compared to lower energies, as discussed in Section D. For the typical case of 110 MeV bombardment the fission cross section is found to be about 15% less than the calculated reaction cross section which could be interpreted by saying that at this energy the fraction of direct interactions which do not lead to fission is about 15% and the calculated reaction cross section is in agreement with the experiment. An alternative explanation for this can be that the optical model calculations give about 15% overestimate of σ_R (and therefore $\langle \ell^2 \rangle$) and there are no direct interactions not leading to fission. However, in either case the corrections to be applied to the values of K_{ol}^2 are the same.

For comparison with the optical model calculations, we have also plotted the values of $\langle \ell^2 \rangle$ in Fig. 7, as calculated from the classical model which is expected to be valid for the large alpha particle bombarding energies. The values of $\langle \ell^2 \rangle$ were calculated from the relationship

$$\langle \ell^2 \rangle = \frac{\ell^2_{max}}{2} = \frac{M(E - V)}{\hbar^2} R^2 \quad , \tag{13}$$

where M is the mass of the alpha particle, V is the Coulomb barrier height and R is taken equal to $(1.5A^{1/3} + 1.2)$.

It can be seen from Fig. 7 that the values of $\langle \ell^2 \rangle$ calculated from the two models are in excellent agreement in the middle range of alpha particle energies. At bombarding energies in the region of 110 MeV, the values of $\langle \ell^2 \rangle$ calculated from the classical model are, in fact, larger by about 5% than those calculated from the optical model. On the basis of the above considerations, there does not appear to be any evidence to show that the value of $\langle \ell^2 \rangle$ may have been overestimated at higher alpha particle energies, thereby resulting in the larger values of K_o^2.

D. Direct Interaction Effect

In the transformation of the angular distribution to the center of mass system and the calculation of $\langle \ell^2 \rangle$, it was assumed for the simplified analysis of the data that the incident alpha particle deposits all its momentum on the target nucleus and forms the compound nucleus. However, the above assumption is not expected to be true for higher bombarding energies, where a significant fraction of the interactions may take place via the mechanism of direct interactions leading to incomplete momentum transfer. The deduced values of K_o^2 can then appear to be larger due to two kinds of effects introduced by the presence of direct interactions. In the first place, the fissions which follow direct interactions can be expected to have different angular distributions as compared to those which follow full momentum transfer. Secondly, even if the nuclei do not undergo fission following direct interactions, the very presence of direct interaction events may effect the values of $\langle \ell^2 \rangle$. In what follows we have estimated the effect of each kind on the deduced values of K_{o1}^2 by considering the case of bombardment by 110 MeV alpha particles. The fraction of fissions which follow direct interactions can be experimentally determined[27] by investigating the forward linear momentum transfer from a study of the fragment-fragment angular correlations. These angular correlations were measured[28] for the cases of fission of Bi^{209} and U^{238} bombarded by 110 MeV alpha particles, and the results are shown in Figs. 9a and 9b. It can be seen from Fig. 9 that the angular correlation for the case of Bi^{209} shows a single symmetric peak with a half width of about 5.5^o. A single symmetric peak is expected for the case of specific momentum transfer followed by symmetric fission and, therefore, it can be inferred that in the case of bombardment of Bi^{209} practically all the observed fissions correspond to the case of full momentum transfer even when the alpha particle energy is as high as 110 MeV. This is what one expects for these less fissile nuclei, where the fission cross section decreases sharply with the decrease in the energy deposited on the nucleus, thereby reducing by a large amount the probability of fission in the case of direct interaction events.

However, for the case of bombardment of U^{238} the observed distribution does indicate the presence of a small secondary peak corresponding to the fissions following incomplete momentum transfer. In this case the fraction of the fissions following direct interactions was determined by

fitting the observed distribution to the sum of two Gaussian distributions by a least-squares fitting code. The two Gaussian distributions which when summed, give the best fit to the observed distribution are also shown in Fig. 9b. From the fractional area under the secondary peak, it is estimated that in this case about 9% of the fission events follow direct interactions. It is expected that the laboratory angular distributions transformed to the center of mass system under the assumption of full momentum transfer will not be appreciably affected due to the presence of this small fraction of the direct interaction events. In fact, the only effect, if any, of taking into account this fraction in the transformation will be to reduce the center of mass anisotropy resulting in a further increase in the value of K_{o1}^2. (This is because the angular distributions are measured mainly in the backward directions; and the assumption of full momentum transfer leads to overcorrection if there are some events with incomplete momentum transfer.)

However, since the fragments in the direct interaction events are expected[29] to have different angular distributions, the deduced values of K_{o1}^2 should be corrected for these background events. Under the reasonable assumptions that the values of N(90)/N(0) for these events is between 1.0 and 3.0, the overestimate[30] in the deduced values of K_o^2 corresponds to between 10% and 16%, respectively. Secondly, the presence of direct interactions not leading to fission can reduce the value of $\langle \ell^2 \rangle$ relevant for the nuclei undergoing fission. This is because the direct interaction, which presumably is a surface reaction, occurs at the expense of compound nucleus formation with large ℓ-values. In the presence of direct interactions, the value $\langle \ell^2 \rangle_c$ relevant for the compound nucleus interactions can be written as

$$\frac{\langle \ell^2 \rangle_c}{\langle \ell^2 \rangle} \approx \frac{\sigma_c}{\sigma_c + \sigma_d} , \qquad (14)$$

where $\langle \ell^2 \rangle$ is the value calculated from the optical model and σ_c, σ_d are the cross sections for the events corresponding to compound nuclei and direct interactions, respectively.

In the case of U^{238}, we find that the fission cross section at 110 MeV is about 15% lower than the total reaction cross section calculated from the optical model. Since at this energy all interactions

with complete momentum transfer are expected to ultimately lead to fission, the above deviation pointing to the formation of spallation products can be interpreted as due to the direct interaction events occurring with a fraction of about 15%. The total fraction of direct interaction events which either lead to fission or spallation products can therefore be estimated to be about 24% (15% + 9%) in this case, implying that the value of $\langle \ell^2 \rangle$ relevant for the compound nucleus interactions is lower by the same value. Therefore, the total direct interaction events which do or do not lead to fission can be expected to give rise to an apparent increase of about 34% (24% + 10%) in the values of K_{ol}^2 at 110 MeV bombarding energy. In order to correct the values of K_{ol}^2 throughout the energy range it has been assumed that the fraction of direct interaction events decreases linearly with the bombarding energy. The closed rectangles in Fig. 6 represent the deduced values of K_{ol}^2 corrected for this estimated direct interaction effect. To bring about clearly the deviations of these corrected values of K_{ol}^2 from the expected Fermi gas dependence, we have shown in Fig. 10 a plot of $K_{ol}^2/(Ex^s)^{\frac{1}{2}}$ versus Ex^s. It is clear from Fig. 10 that $K_{ol}^2/(Ex^s)^{\frac{1}{2}}$, instead of being constant, increases significantly with Ex^s.

E. General Discussion

From the analysis of the results in the case of Pu^{242} fission, where it has been possible to correct the data for the known complexities, it is clear that K_{ol}^2 does not seem to vary with Ex^s as expected on the statistical theory (Fig. 10). The same trend is found in the case of fission of Bi^{209}, where for the typical case of bombardment with 110 MeV alpha particles the deduced value of K_o^2 is found to be at least 30% larger than expected. In this case also the corrections for the multichance fissions and the ℓ-dependence of fissionability should further increase the values of first chance K_{ol}^2, especially at higher energies. The energy dependence of $K_o^2/(Ex^s)^{\frac{1}{2}}$ was also indicated from the angular distribution measurements of Viola, et. al.[31] in the case of heavy-ion induced fission of bismuth and gold. It is very likely that in their work also only a part of the observed disagreement with the theory might have arisen from the direct interaction effects, and their results also indicated a genuine deviation from theory. In what

follows the various possible reasons leading to the observed deviations from the predictions of a simple Fermi gas model are discussed.

As seen from Fig. 6, it is possible to explain the present results, if K_{o1}^2 is assumed to be proportional to Ex^s rather than $(Ex^s)^{\frac{1}{2}}$. This would imply that either the distribution of K states at the saddle point is determined from considerations other than that suggested by Halpern and Strutinski,[3] or the saddle point nuclear temperature has a linear dependence on Ex^s rather than the square root dependence given by the Fermi gas model. Although the known linear dependence of K_o^2 on Ex^s for low values of Ex^s has been explained on the basis of nuclear pairing effects,[18] it can be said that the same linear dependence persists throughout the energy range of Ex^s even after the pairing effects have presumably died out.

On the other hand if the Fermi gas dependence of K_o^2 on Ex^s is assumed to be true, the present results can be explained if one assumes that $J_{eff}/a_f^{\frac{1}{2}}$ increases with the excitation energy or with the increasing angular momentum as shown in Fig. 10. If the decrease of a_f with the excitation energy is not expected, which appears reasonable, one has to infer that J_{eff} is increasing with excitation energy or angular momentum. The increase in J_{eff} can be expected for values of Ex^s up to about 20 MeV on the basis of disappearance of the pairing effects with the increasing excitation energy. For higher excitation energies, where a rigid body value of J_{eff} is assumed, a change in J_{eff} should involve some other effect.

An increase in the value of J_{eff} with excitation energy may be expected to come about due to the presence of wriggling and bending modes of oscillations about the saddle point shapes as described by Nix and Swiatecki.[32] Since these modes are not axially symmetric, their presence should on the average increase $J_{\parallel}$ and decrease $J_{\perp}$, resulting in an increase in the value of J_{eff}. Qualitatively, it is therefore expected that J_{eff} should increase with excitation energy as the result of an increase in the intensity of these oscillations with nuclear temperature. However, some quantitative estimates made by Nix[33] show that the increase in J_{eff} due to these effects is only about 2% when the nuclear temperature is increased from 0 to 2 MeV; therefore, this effect can be ruled out as a possible reason for the observed increase in J_{eff}.

The rapid increase in the value of J_{eff} with the bombarding energy can be interpreted to suggest that the saddle point shape of the nucleus changes significantly with the increasing angular momentum ℓ. Although a dependence of the saddle shape on the angular momentum is expected on the basis of the liquid drop calculations,[12] the results of these calculations show a much weaker dependence on the rotational energy than required to explain the results shown in Fig. 10. For example, these calculations show an increase in the value of J_{eff} of only about 9% for Pu^{242}, and of only about 5% for the case of At^{213} in going from zero rotational energy to the values corresponding to the 115 MeV alpha bombardment. In Fig. 10, the rotational energy $E_R^{\,o}$ of the initial spherical nucleus is shown in terms of the dimensionless parameter $y = E_R^{\,o}/E_s^{\,o}$, where the surface energy $E_s^{\,o}$ is taken equal to 17.8 $A^{2/3}$ (MeV). If the observed deviations are attributed entirely to the angular momentum effect, the present results show that for the case of Pu^{242}, J_{eff} is nearly doubled in value in going from $y = 0$ to $y = 0.0058(\langle\ell^2\rangle_e = 1060)$. Comparing this with the results of rotating liquid drop calculations, one finds that the observed increase of J_{eff} with rotational energy has to be about ten times more rapid than that given by these calculations.

It is known[5] that the observed values of J_{eff} are found to increase more rapidly with Z^2/A than expected on the basis of the above calculations for values of Z^2/A greater than about 33. It has been suggested by Strutinski[34] that if a curvature correction term to the surface energy is included in the calculations, the variation of J_{eff} with Z^2/A can be made more rapid (and therefore in accordance with the deduced values) for the range of Z^2/A greater than about 33. It is shown in the Appendix that if the slope of J_{eff} versus Z^2/A is modified by incorporating some changes in the surface energy term, the natural consequence is that the slope of J_{eff} versus y is also changed in the same ratio. Therefore, in the region of Z^2/A corresponding to Pu^{242}, if it is assumed that J_{eff} increases about ten times more rapidly with Z^2/A than the increase given by the above calculations, one can expect an equally more rapid increase in J_{eff} with angular momentum as compared to the above calculated results. Though the variation of J_{eff} with Z^2/A as deduced by Reising, et. al.[5] does appear to be more rapid than the calculated one, it is difficult to infer the exact slope, due to the presence of scatter in the deduced

values. In any case, the difference in the slopes of the experimental and calculated variation of J_{eff} with Z^2/A indicates at least qualitatively a significantly more rapid increase of J_{eff} with angular momentum than the calculated one.

If the observed deviation in the values of K_o^2 with the theory is not fully attributable to the effects mentioned above, this would imply that certain assumptions of the theory may not be true, especially at higher energies. In particular, if the time the nucleus spends in passing over the barrier becomes comparable with the nuclear period, so that the states at the saddle point are not even quasi-stationary, the spectrum of states at the saddle may have little physical significance even in the statistical approach. In such a case a somewhat weaker correlation may exist between the angular momentum axis and the fission axis, thereby resulting in a lower anisotropy and consequently apparently larger values of K_o^2. However, within the framework of the statistical approach of Halpern and Strutinski it is most reasonable to infer that either J_{eff} increases too rapidly with the angular momentum or the relationship between the saddle point excitation energy and the nuclear temperature is different from that given by the Fermi gas dependence.

ACKNOWLEDGMENTS

We are very much thankful to Dr. Franz Plasil for his active participation in the early part of this work. Our thanks are also due to Dr. H. C. Britt of the Los Alamos Scientific Laboratory for helpful discussions and for providing us with uranium foils. We are sincerely indebted to Dr. Wladyslaw J. Swiatecki for several useful discussions which have greatly contributed towards this work. It is a pleasure to acknowledge the helpful discussions with Dr. Robert Vandenbosch, Dr. I. Halpern, Dr. J. R. Huizenga, Dr. J. R. Nix and Dr. A. Gilbert.

We are extremely thankful to Claudette Rugge for her contribution to this work in writing up the least-squares fitting programs to the theoretical functions and for carrying out all activities directly concerned with the computers. Thanks are due to Bernard G. Harvey and the staff of the 88-in. cyclotron for help and cooperation with the experimental work. The help of Mr. A. Khodai in the last phases of the experimental work is gratefully acknowledged. Our thanks go to Daniel J. O'Connell for preparing the targets used in this work. We gratefully acknowledge the valuable assistance of Joan Phillips in preparing the manuscript. One of us (S. S. Kapoor) wishes to express his thanks to the Agency for International Development, Washington, the Atomic Energy Establishment, Trombay, the Lawrence Radiation Laboratory, Berkeley and the U. S. Atomic Energy Commission for providing the opportunity to work at the Lawrence Radiation Laboratory, Berkeley.

APPENDIX

Variation of J_{eff} with Z^2/A and Angular Momentum ℓ[35]

The variations of J_{eff} with nuclear charge (i.e. Z^2/A) and with angular momentum ℓ may be related to each other by making use of the fact that under certain circumstances (i.e., when dealing with fairly elongated shapes) the electrostatic repulsion and the centrifugal forces are fairly similar in their effects in modifying the shape of a nucleus. (The principle tendency of both effects is to tear apart an elongated nucleus into fragments.) In fact, if the presence of rotation (i.e., the presence of angular momentum ℓ) can be simulated by an increase in the amount of charge (i.e., an increase in Z^2/A) it follows that any anomalies present in the plots of J_{eff} (or any other quantity related to deformation) against Z^2/A should have their counterpart anomalies in plots against ℓ.

One can bring about the above argument quantitatively in the following manner. It is assumed here that both the Coulombic and centrifugal forces produce a single family of shapes characterized by a deformation parameter θ.

The total deformation energy E_d of a nucleus as a function of deformation parameter θ can be written as

$$E_d(\theta) = E_s - E_s^{\,o} + E_c - E_c^{\,o} + E_R - E_R^{\,o} \quad , \tag{A1}$$

where E_s, E_c and E_R are, respectively, the surface, Coulomb and rotational energies for the deformed nucleus and $E_s^{\,o}$, $E_c^{\,o}$ and $E_R^{\,o}$ are the corresponding quantities for the original spherical nucleus. The deformation energy in units of the surface energy $E_s^{\,o}$ can be written as

$$\frac{E_d(\theta)}{E_s^{\,o}} \equiv \xi(\theta) = (B_s - 1) + 2x(B_c - 1) + y(B_R - 1) \tag{A2}$$

$$\equiv F(\theta) + 2x\, G(\theta) + y\, H(\theta) \quad , \tag{A3}$$

where $B_s = E_s/E_s^{\,o}$, $B_c = E_c/E_c^{\,o}$, $B_R = E_R/E_R^{\,o}$, $x = E_c/2E_s^{\,o} \equiv (Z^2/A)/(Z^2/A)_c$ and $y = E_R^{\,o}/E_s^{\,o}$. The saddle shape is obtained from the relation

$$F'(\theta) + 2x\, G'(\theta) + y\, H'(\theta) = 0 \quad . \tag{A4}$$

Differentiating Eq. (A4) with respect to x and y, one gets

$$\frac{d\theta}{dx} = \frac{-2\,G'(\theta)}{F''(\theta) + 2x\,G''(\theta) + y\,H''(\theta)} \tag{A5}$$

and

$$\frac{d\theta}{dx} = \frac{-\,H'(\theta)}{F''(\theta) + 2x\,G''(\theta) + y\,H''(\theta)} \quad . \tag{A6}$$

The variation of J_{eff} can be written in the form,

$$\frac{d(J_{eff})}{dx} = \frac{d(J_{eff})}{d\theta}\,\frac{d\theta}{dx} \quad , \tag{A7}$$

and

$$\frac{d(J_{eff})}{dy} = \frac{d(J_{eff})}{d\theta}\,\frac{d\theta}{dy} \quad . \tag{A8}$$

It follows from Eqs. (A7) and (A8) that

$$\frac{\dfrac{d(J_{eff})}{dx}}{\dfrac{d(J_{eff})}{dy}} = \frac{2G'(\theta)}{H'(\theta)} = \text{const (independent of surface energy)} \tag{A9}$$

On the basis of Eq. (A9) if the surface energy term in the liquid drop calculations is modified in order to change the slope $d(J_{eff})/dx$, as a result of this, the slope $d(J_{eff})/dy$ will also get changed in the same ratio. In particular, if the inclusion of curvature correction[34] in the calculations leads to a more rapid variation of J_{eff} with Z^2/A, it should also give a more rapid variation of J_{eff} with ℓ.

FOOTNOTES AND REFERENCES

* This work was done under the auspices of the U. S. Atomic Energy Commission.

† Present address: Nuclear Physics Division, Atomic Energy Establishment, Trombay, Bombay, India.

‡ Present address: Japan Atomic Energy Research Institute, Tokai-mura, Ibaraki-ken, Japan.

1. G. E. Gindler and J. R. Huizenga, Nuclear Fission, 1965 (to be published).
2. A. Bohr, in Proceedings of the First United Nations International Conference on the Peaceful Uses of Atomic Energy, Geneva, 1955 (United Nations, Geneva, 1956), Vol. 2, p. 151.
3. I. Halpern and V. M. Strutinski, in Proceedings of the Second United Nations International Conference on the Peaceful Uses of Atomic Energy, Geneva, 1958 (United Nations, Geneva, 1958), Vol. 15, p. 408.
4. J. J. Griffin, Phys. Rev. 116, 107 (1959); Phys. Rev. 127, 1248 (1962); Phys. Rev. 134, B817 (1964).
5. R. F. Reising, G. L. Bate and J. R. Huizenga, Phys. Rev. 141, 1161 (1966).
6. Elmer L. Kelly, University of California Lawrence Radiation Laboratory Report UCRL-10081, 1962 (unpublished).
7. T. Sikkeland, E. L. Haines and V. E. Viola, Phys. Rev. 125, 1350 (1962).
8. R. Vandenbosch, H. Warhanek and J. R. Huizenga, Phys. Rev. 124, 846 (1961).
9. R. B. Leachman and L. Blumberg, Phys. Rev. 137, B814 (1965).
10. F. Everling, L. A. König, J. H. E. Mattauch and A. H. Wapstra, Nucl. Phys. 18, 529 (1960).
11. F. Plasil (Ph.D. Thesis), University of California Lawrence Radiation Laboratory Report UCRL-11193, Dec. 1963 (unpublished).
12. S. Cohen, F. Plasil and W. J. Swiatecki, University of California Lawrence Radiation Laboratory Report UCRL-10775, April 1963 (unpublished), and continuation of this work to be published; S. Cohen and W. J. Swiatecki, Ann. Phys. 22, 406 (1963).
13. W. Myers and W. J. Swiatecki, University of California Lawrence Radiation Laboratory Report UCRL-11980, May 1965 (unpublished).
14. R. Chaudhry, R. Vandenbosch and J. R. Huizenga, Phys. Rev. 126, 220 (1962).

15. For the sake of consistency, their results are also plotted at the value of Ex^s obtained using the calculated value of 16.2 MeV for the fission barrier height instead of 15.8 MeV as used by them.

16. J. E. Simmons, R. B. Perkins and R. L. Henkel, Phys. Rev. 137, B809 (1965).

17. V. E. Viola, Jr., J. M. Alexander and A. R. Trips, Phys. Rev. 138, B1434 (1965).

18. J. J. Griffin, Phys. Rev. 132, 2204 (1963).

19. R. Vandenbosch, private communication.

20. J. R. Huizenga and R. Vandenbosch, in Nuclear Reactions, edited by P. M. Endt and P. B. Smith (North Holland Publishing Co., Amsterdam, 1962), p. 42.

21. We are thankful to Dr. N. Glendenning of this laboratory for making use of his optical model program.

22. J. R. Huizenga and G. Igo, Nucl. Phys. 29, 462 (1962).

23. J. R. Huizenga, R. Vandenbosch and H. Warhanek, Phys. Rev. 124, 1964 (1961).

24. The fission cross section σ_f was calculated by integrating the measured angular distributions $(d\sigma/d\Omega)_\theta$ over all the solid angles.

$$\sigma_f = 2\pi\ (d\sigma/d\Omega)_{90^\circ} \int_0^\pi \frac{(d\sigma/d\Omega)_\theta}{(d\sigma/d\Omega)_{90}} \sin\theta\ d\theta \quad ,$$

where $(d\sigma/d\Omega)_{90^\circ}$ is obtained from the measured counts at 90°, total beam current, effective target thickness and the solid angle subtended by the detector. The solid angle subtended by the detector was experimentally measured using a standardized point source of Am^{241}.

25. V. E. Viola, Jr. and T. Sikkeland, University of California Lawrence Radiation Laboratory Report UCRL-10088, February 1962 (unpublished).

26. J. Wing, W. J. Ramler, A. L. Harkness and J. R. Huizenga, Phys. Rev. 114, 163 (1959).

27. T. Sikkeland, E. L. Haines and V. E. Viola, Jr., Phys. Rev. 125, 1350 (1962).

28. In these measurements one of the detectors was kept fixed at 90° to the beam direction and fragment-fragment coincidences were counted for different angular positions of the second detector placed on the other side of the foil. The angular spread in these measurements as defined by the size of the collimator in front of the detectors was ±1/3°.

29. Although in these events also forward-backward anisotropy results with respect to the recoil axis of the nucleus, the distribution with respect to the incident beam after averaging over all possible nucleus recoil directions should result in an angular distribution different from the case of full momentum transfer.

30. For values of p close to 1, the change Δp in parameter p due to the change ΔA in anisotropy A is given by

$$\frac{\Delta p}{p} \sim \frac{A}{A - 1} \cdot \frac{\Delta A}{A} \quad .$$

For $A \sim 1.5$, $\Delta p/p \sim 3\Delta A/A$.

31. Victor E. Viola, Jr., T. D. Thomas and G. T. Seaborg, Phys. Rev. 129, 2710 (1963).

32. J. R. Nix and W. J. Swiatecki, Nucl. Phys. 71, 1 (1965).

33. We are thankful to J. R. Nix for communicating the results of these calculations.

34. V. M. Strutinski, I. V. Kurchatov Atomic Energy Institute, Moscow, Preprint IAE-735, pp. 1-7 (1964); [translation: Argonne National Laboratory Translation 157].

35. The contents of this section are primarily due to the suggestions and work by Dr. W. J. Swiatecki.

FIGURE CAPTIONS

Fig. 1. Relative differential cross-section as a function of the center of mass angle in degrees. The open and the closed points represent the experimental data taken in the backward and the forward directions, respectively. The solid curve is the Legendre polynomial fit to the data. The dotted curve represents the least square fit of the data to Eq. (4) to deduce the value of P ($= \langle \ell^2 \rangle / 2K_o^2$).

Fig. 2. The center of mass fragment anisotropies versus bombarding energy of alpha particles in the alpha induced fission of U^{238}.

Fig. 3. The deduced values of K_o^2 as a function of the excitation energy Ex^s above the fission barrier for the case of alpha induced fission of Bi^{209}. The values of K_o^2 obtained by Chaudhry, et. al.[13] for the relatively low energy region are also shown. The shaded region represents the dependence expected on the Fermi gas model as obtained by normalizing to the value of K_o^2 for the case of 40 MeV alpha bombarding energy where essentially all the observed fissions correspond to the first chance fissions.

Fig. 4. The deduced values of K_o^2 as a function of the excitation energy Ex^s above the fission barrier for the case of alpha induced fission of U^{238}. The two points shown by triangle and closed circle represent the values obtained by Simmons, et. al.[15] and Viola, et. al.[16] The dotted curve has been drawn through the experimental points in a smooth fashion to represent the observed variation of K_o^2 with Ex^s.

Fig. 5. A plot of $K_o^2/(Ex^s)^{\frac{1}{2}}$ versus Ex^s for the case of alpha induced fission of U^{238}.

Fig. 6. The extracted values of the first chance fission K_o^2 (denoted by K_{o1}^2) versus Ex^s. The values of K_{o1}^2 are extracted under the assumption that $a_n = a_f = A/\beta$. The circle, cross and triangle represent the values of K_{o1}^2 deduced for values of β equal to 8, 15 and 20, respectively. The values of K_{o1}^2 are best represented by the rectangles enclosing the three points, where the experimental uncertainty in the values of K_{o1}^2 are also included. The values of K_{o1}^2 corrected for the estimated maximum direct interaction effects are shown as closed bars.

Fig. 7. Values of $\langle \ell^2 \rangle$ for different alpha particle bombarding energies calculated with the optical model code using the Woods-Saxon parameters as listed in the figure. The dotted and the solid curves correspond to the target nuclei of Bi^{209} and U^{238}, respectively. The classical model values of $\langle \ell^2 \rangle$ calculated with $R_o = (1.5\ A^{1/3} + 1.2)$ are shown as circles and triangles for the case of Bi^{209} and U^{238}, respectively.

Fig. 8a. Measured fission cross sections at different alpha bombarding energies for the case of alpha induced fission of U^{238}. The reaction cross sections calculated from optical model code are shown by the solid line curve.

b. The ratio of the measured fission cross sections to the calculated reaction cross sections for different alpha bombarding energies. The closed circles represent the measurements carried out in this work.

Fig. 9. The measured fragment-fragment angular correlation for the case of alpha induced fission of (a) Bi^{209} and (b) U^{238}. The number of fragment-fragment coincidences is plotted for various angular positions of one of the detectors with respect to the beam direction, while the second detector is kept at a fixed angle of 90° with the beam on the other side of the foil. For the case of target nucleus U^{238} (Fig. b), the best fit to the observed distribution is obtained by the sum of two Gaussian distributions represented by solid line curves in the figure. From the area under the secondary small Gaussian peak, the percentage of fissions following incomplete momentum transfer is inferred.

Fig. 10. A plot of $K_{o1}^2/(Ex^s)^{\frac{1}{2}}$ versus Ex^s. K_{o1}^2 are values of K_o^2 extracted for first chance fission at saddle point excitation energy Ex^s. These values of K_{o1}^2 have been further corrected for the estimated maximum direct interaction effects. On the Fermi gas model, this can also be written as a plot of $J_{eff}/\hbar^2 \cdot a_f^{\frac{1}{2}}$ versus Ex^s. The values of the average angular momenta of the fissioning nucleus are shown on the top x-axis in terms of rotational parameter y, where y is the ratio of the rotational energy E_R^o to the surface energy E_s^o for the initial spherical shape of the nucleus. The surface energy E_s^o is taken as equal to $17.8\ A^{2/3}$ (MeV).

Table I. Summary of the experimental results on the angular distributions of the fragments in the alpha induced fission of Bi^{209} and U^{238}. The center of mass anisotropies and the coefficients of the Legendre Polynomials obtained from the least square fit to the angular distributions are listed for various alpha particle bombarding energies. $N(\theta) = 1 + \sum_n \alpha_{2n} P_{2n} (\cos \theta)$.

E_α (MeV)	Bi^{209} N(171)/N(90)	α_2	α_4	α_6	α_8	α_{10}	U^{238} N(171)/N(90)	α_2	α_4	α_6	α_8	α_{10}
23.3[a]							1.17±0.03[b]	0.119±0.008[c]	0.031±0.009	0.011±0.010	-0.002±0.012	
30.0							1.36±0.04	0.114±0.005	0.017±0.007	0.011±0.008		
40.0	2.10±0.08[b]	0.480±0.018[c]	0.119±0.022	-0.001±0.025			1.51±0.04	0.254±0.005	0.033±0.007	0.009±0.008	0.004±0.010	
50.0	2.12±0.05	0.470±0.006	0.127±0.009	0.044±0.010	-0.006±0.011	0.019±0.012	1.54±0.04	0.264±0.003	0.024±0.003	0.011±0.004	-0.002±0.004	0.001±0.005
60.0	2.27±0.05	0.512±0.005	0.186±0.006	0.042±0.007	0.005±0.009		1.60±0.04	0.291±0.003	0.055±0.004	0.008±0.005	-0.006±0.005	-0.002±0.006
70.0	2.36±0.06	0.527±0.007	0.139±0.009	0.043±0.010	0.004±0.012		1.60±0.04	0.277±0.002	0.048±0.003	0.026±0.004	-0.002±0.004	
80.0	2.44±0.06	0.549±0.005	0.196±0.006	0.055±0.008	0.025±0.009	0.011±0.010	1.56±0.05	0.271±0.005	0.061±0.007	0.012±0.008	-0.004±0.010	0.003±0.011
85.0							1.61±0.05	0.293±0.002	0.020±0.003	0.016±0.003	-0.006±0.004	-0.010±0.004
90.0	2.46±0.06	0.556±0.003	0.190±0.004	0.053±0.005	0.001±0.005		1.60±0.04	0.284±0.007	0.059±0.009	0.014±0.011	-0.010±0.012	-0.014±0 013
100.0	2.46±0.06	0.566±0.004	0.210±0.005	0.048±0.005	0.005±0.007	-0.003±0.007	1.58±0.04	0.284±0.003	0.046±0.004	0.005±0.004		
110.0	2.48±0.06	0.550±0.006	0.208±0.008	0.072±0.009	0.007±0.010	0.005±0.012	1.60±0.04	0.284±0.005	0.053±0.006	0.016±0.007	-0.002±0.008	
115.0	2.49±0.06	0.562±0.004	0.184±0.005	0.062±0.005	0.017±0.006	-0.003±0.007	1.57±0.04	0.280±0.002	0.054±0.003	0.003±0.003	0.004±0.004	-0.001±0.004

[a] These energies of the alpha particles are calculated from the stated operating conditions of the cyclotron. The error in these energies is expected to be less than 0.5%.

[b] Includes systematic errors in addition to statistical errors.

[c] These errors correspond to the standard deviations in the coefficients obtained from the least square fitting code.

Table II. Values of K_o^2 obtained by the least square fit of the observed angular distributions to the theoretical expression (4) and (6) for the various cases. Ex, $\langle \ell^2 \rangle$, E_R^o, E_{PP} and Ex^s are all defined in the text. The rotational energy E_R^o for a spherical nucleus is calculated using r_o = 1.216 F.

				Bi^{209}		K_o^2	
E_α (MeV)	Ex (MeV)	$\langle \ell^2 \rangle$	E_R^o (MeV)	E_{PP} (MeV)	Ex^s (MeV)	Eq. (4)	Eq. (6)
23.3							
30.0							
40.0	30.0	197.5	0.9	12.1	13.4	49.0±0.8[a]	49.5±0.8[a]
50.0	39.8	295.0	1.4	11.8	23.0	75.5±0.8	76.0±0.8
60.0	49.6	393.3	1.8	11.5	32.7	86.8±1.0	87.4±1.0
70.0	59.4	490.0	2.3	11.2	42.3	94.3±1.0	95.0±1.0
80.0	69.2	583.7	2.7	11.0	52.0	112.7±0.8	113.5±0.8
90.0	79.0	677.3	3.1	10.7	61.6	123.1±0.4	124.0±0.4
100.0	88.8	769.8	3.5	10.4	71.3	140.9±0.9	142.0±0.9
110.0	98.6	861.5	3.9	10.2	81.0	158.4±1.1	159.9±1.1
115.0	103.6	907.0	4.1	10.0	85.9	161.3±0.6	162.8±0.6

[a]These errors correspond to the standard deviations in the values of K_o^2 obtained from the least square fitting code and do not include any systematic errors.

Table III. Values of K_o^2 obtained by the least square fit of the observed angular distributions to the theoretical expressions (4) and (6) for the case of alpha induced fission of U^{238}. Ex, $\langle \ell^2 \rangle$, E_B and Ex^s are all defined in the text. $\langle \ell^2 \rangle_e$ is the average square of the angular momentum for the nuclei undergoing fission, as calculated from Eq. (8). K_{ol}^2 is the first chance fission value of K_o^2 extracted using Eq. (11). The values of $\langle \ell^2 \rangle_e$ and K_{ol}^2 are listed for different values of the parameter β defined by $a_n = a_f = A/\beta$.

E_α (MeV)	Ex (MeV)	$\langle \ell^2 \rangle$	E_R^o (MeV)	E_B (MeV)	Ex^s (MeV)	K_o^2 Eq. (4)	K_o^2 Eq. (6)	$\langle \ell^2 \rangle_e$ β=8	$\langle \ell^2 \rangle_e$ β=15	$\langle \ell^2 \rangle_e$ β=23	K_{ol}^2 β=8	K_{ol}^2 β=15	K_{ol}^2 β=23
23.3	17.8	32.8	0.2	4.8	12.9	63.8±3.6[a]	63.0±3.6	33	33	33	64	66	68
30.0	24.5	89.0	0.3	4.7	19.5	74.9±2.4	74.0±2.4	90	90	91	79	84	89
40.0	34.3	194.6	0.7	4.6	29.0	113.1±2.1	112.3±2.1	199	200	201	119	124	130
50.0	44.1	300.9	1.2	4.5	38.4	159.5±3.0	158.8±3.0	311	314	314	169	176	183
60.0	54.0	405.9	1.5	4.2	48.3	200.5±2.4	200.1±2.4	424	428	429	214	222	229
70.0	63.8	509.5	1.9	4.0	57.9	256.8±4.3	256.0±4.3	539	544	544	277	285	292
80.0	73.6	612.3	2.3	3.8	67.5	334.5±9.5	333.5±9.5	650	658	660	362	374	384
85.0	78.5	663.1	2.5	3.7	72.3	309.0±8.2	308.1±8.2	707	716	718	335	346	355
90.0	83.5	713.7	2.7	3.6	77.2	362.7±8.2	362.0±8.2	764	774	776	395	408	418
100.0	93.3	814.4	3.1	3.4	86.8	417.2±5.0	416.8±5.0	878	890	892	457	472	483
110.0	103.1	914.1	3.5	3.3	96.3	457.1±8.0	455.7±8.0	991	1006	1009	502	519	530
115.0	108.1	963.6	3.7	3.2	101.2	515.8±8.1	514.8±8.1	1048	1064	1067	569	587	600

[a]These errors correspond to the standard deviations in the values of K_o^2 obtained from the least square fitting code, and do not include any systematic errors.

Table IV. Values of K_o^2 for the various nuclei formed during the cascade of neutron emission in the 110 MeV alpha bombardment of Bi^{209} as calculated from the relation $K_o^2 = J_{eff} \cdot T/\hbar^2$. The values of $J_{eff}/\hbar^2$ for various mass numbers are obtained by interpolation of the results on the values of $J_{eff}/\hbar^2$ versus Z^2/A as given by Reising, et. al.[5] The saddle-point temperature T is calculated from Ex^s taking $a = A/8$.

Mass No.	Z^2/A	$J_{eff}/\hbar^2$	Ex (MeV)	E_B^* (MeV)	Ex^s (MeV)	T (MeV)	K_o^2
213	33.92	69.9	98.6	13.7	81.0	1.75	122.3
212	34.08	71.8	89.0	15.0	70.1	1.62	116.3
211	34.24	73.6	80.5	15.7	60.9	1.51	111.1
210	34.40	75.5	69.4	15.5	50.0	1.37	103.4
209	34.57	77.4	58.9	14.3	40.7	1.24	96.0
208	34.73	79.2	47.6	13.6	30.1	1.06	84.0
207	34.90	81.1	37.6	12.9	20.8	0.89	72.2
206	35.07	83.0	26.4	11.7	10.8	0.64	53.1
Expt. Value							158.4±5.0

*These values refer to the angular momentum dependent fission barrier height obtained by adding the shell correction term Δ to E_{PP}.

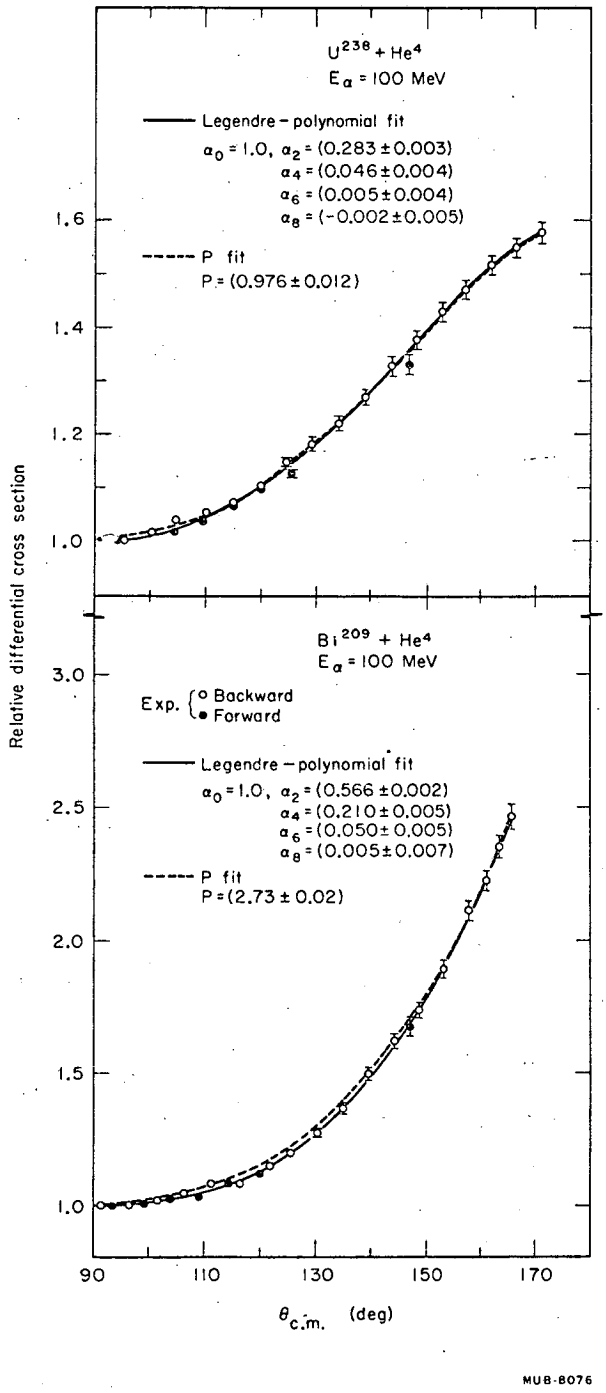
U238 + He4
Eα = 100 MeV
Legendre – polynomial fit
α0 = 1.0, α2 = (0.283 ± 0.003)
α4 = (0.046 ± 0.004)
α6 = (0.005 ± 0.004)
α8 = (-0.002 ± 0.005)
P fit
P = (0.976 ± 0.012)
Bi209 + He4
Eα = 100 MeV
Exp. Backward
Forward
Legendre – polynomial fit
α0 = 1.0, α2 = (0.566 ± 0.002)
α4 = (0.210 ± 0.005)
α6 = (0.050 ± 0.005)
α8 = (0.005 ± 0.007)
P fit
P = (2.73 ± 0.02)
Relative differential cross section
θc.m. (deg)
MUB-8076

Fig. 1

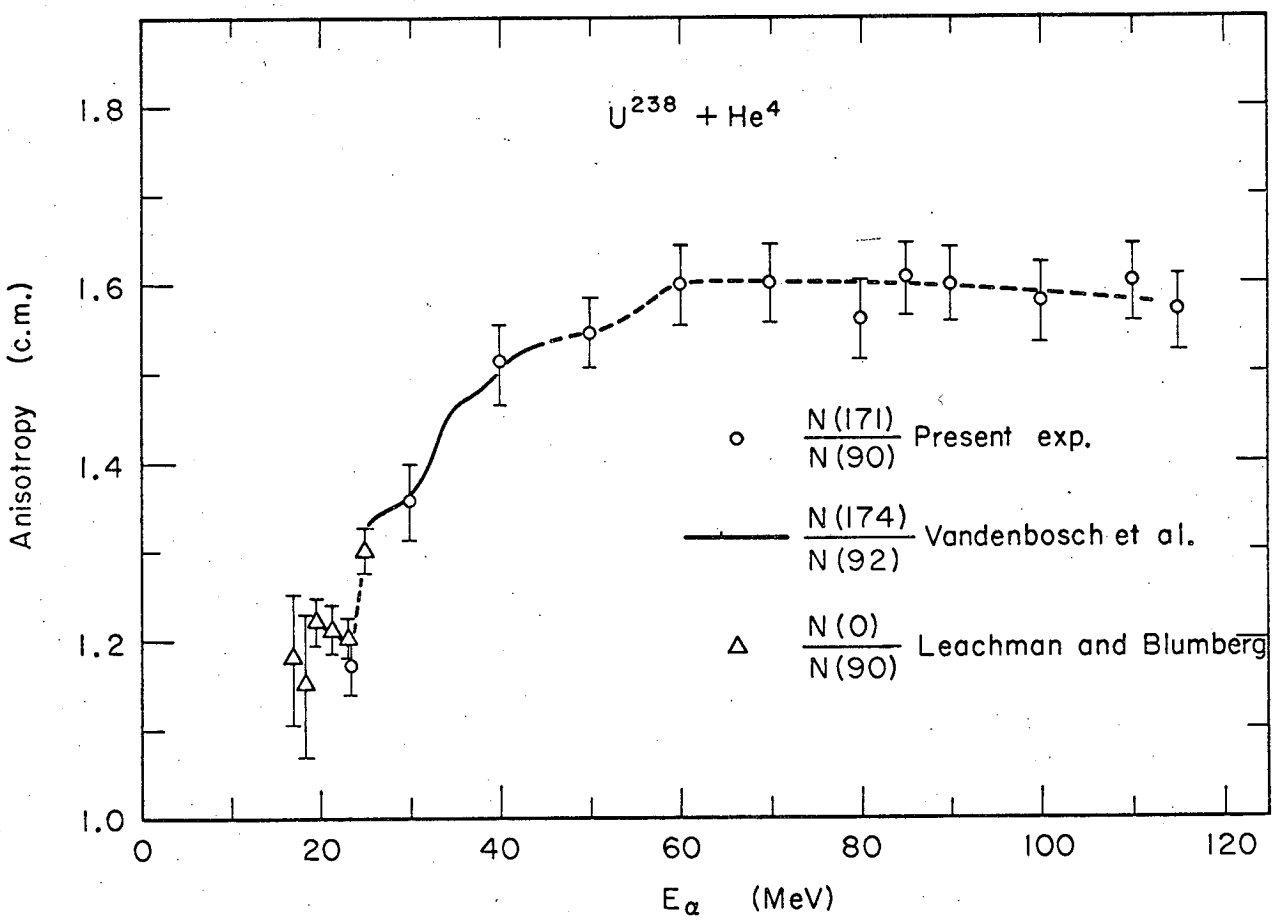

MUB-8079

Fig. 2

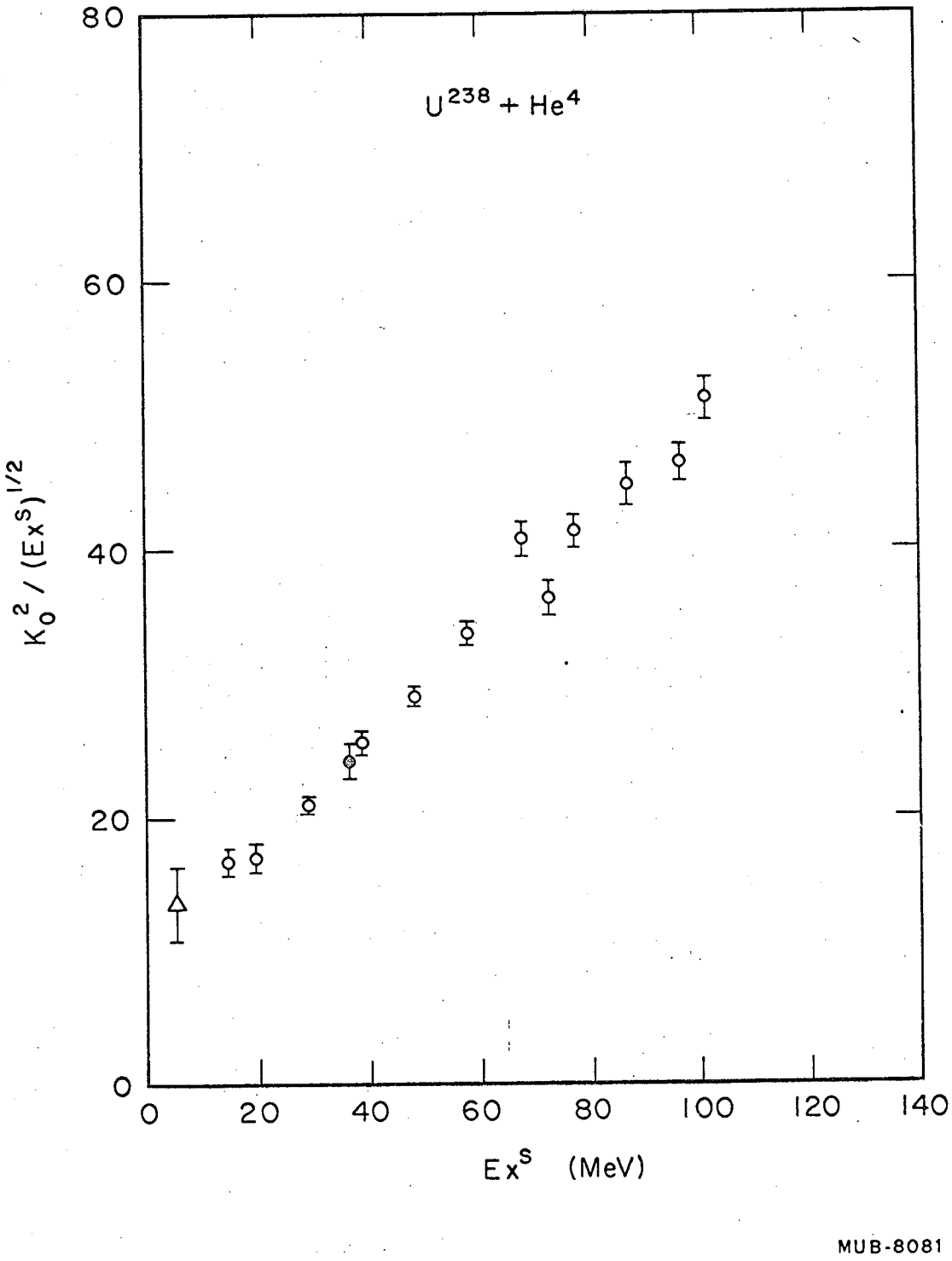

Fig. 5

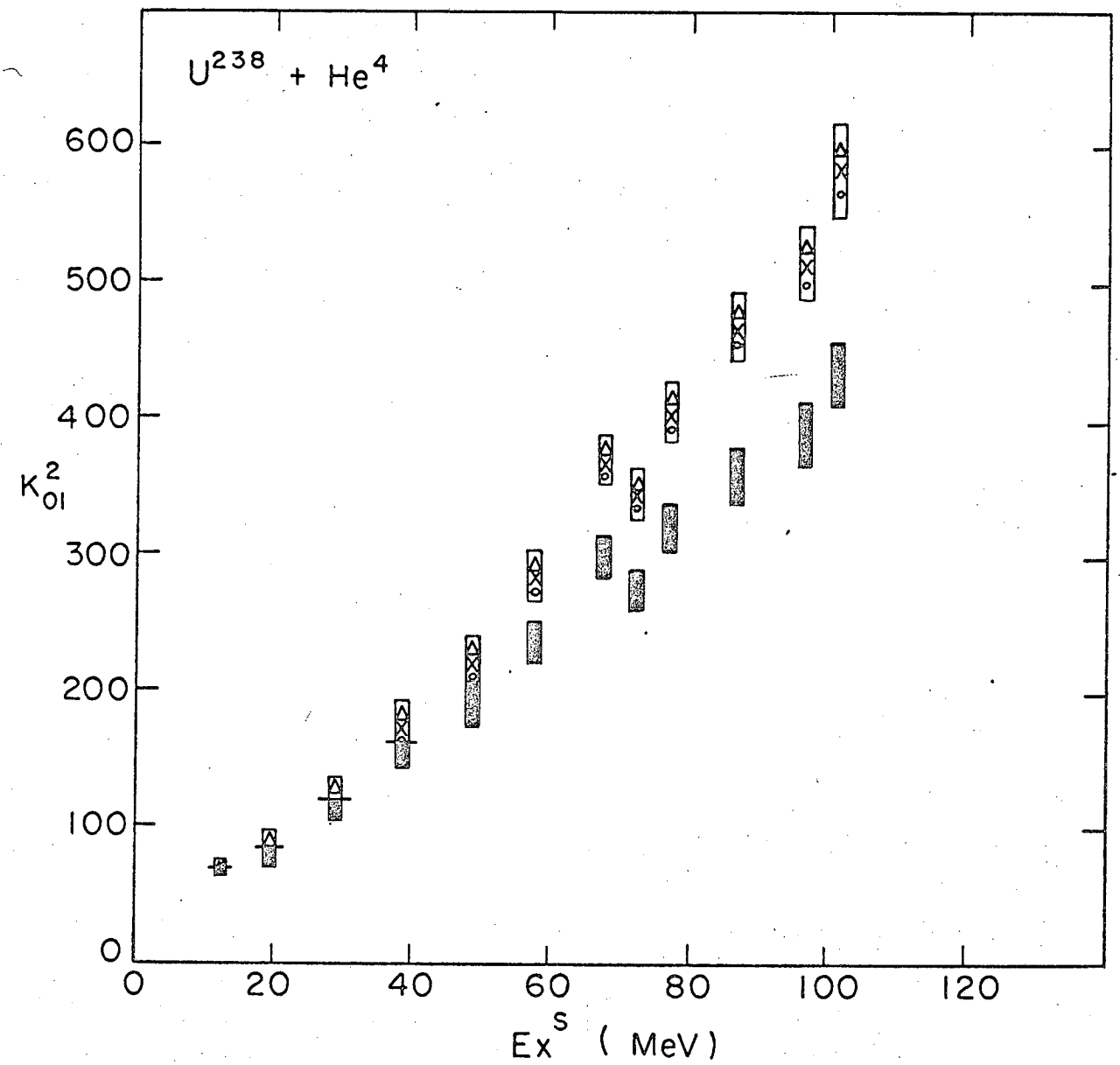

MUB-9487

Fig. 6

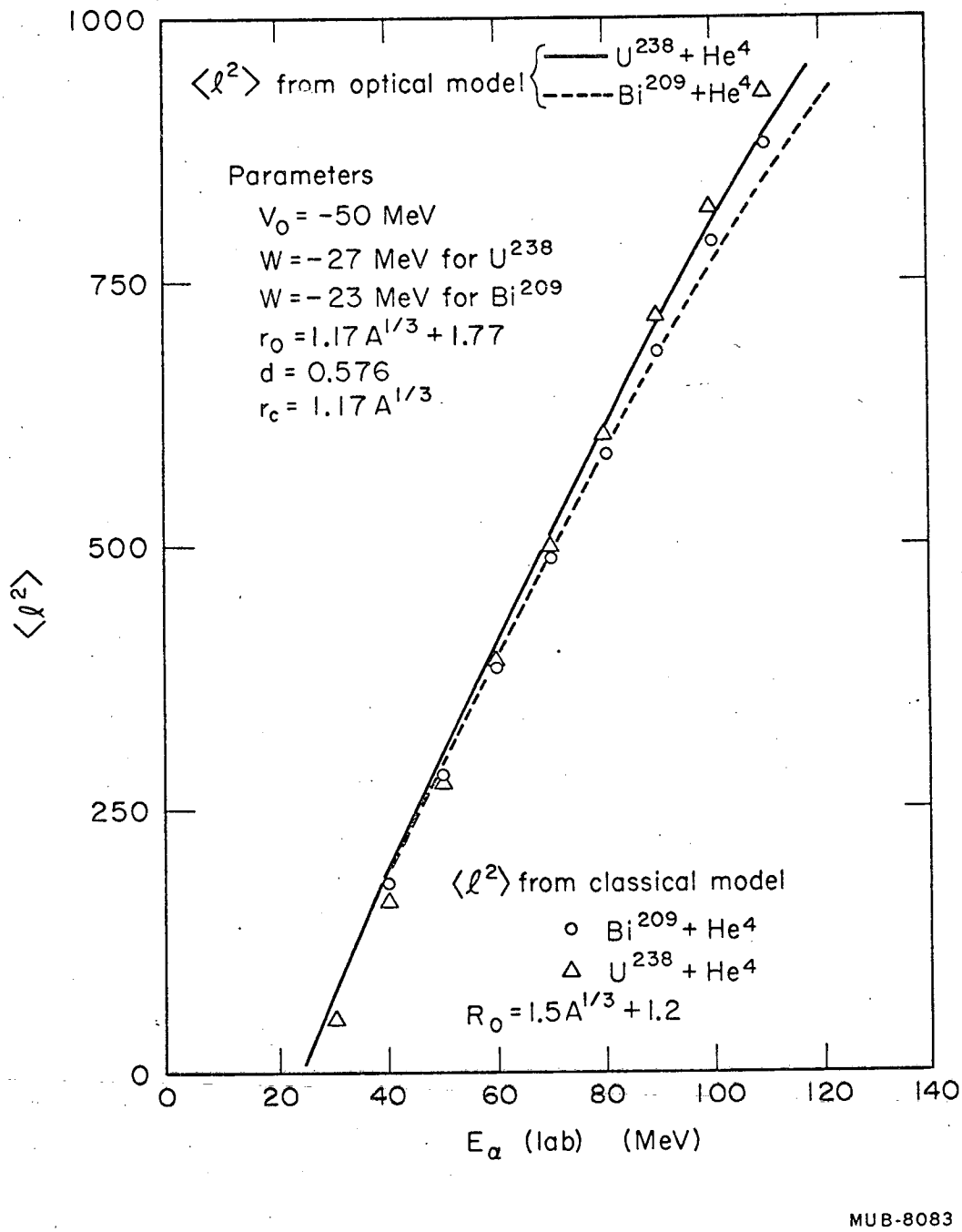

MUB-8083

Fig. 7

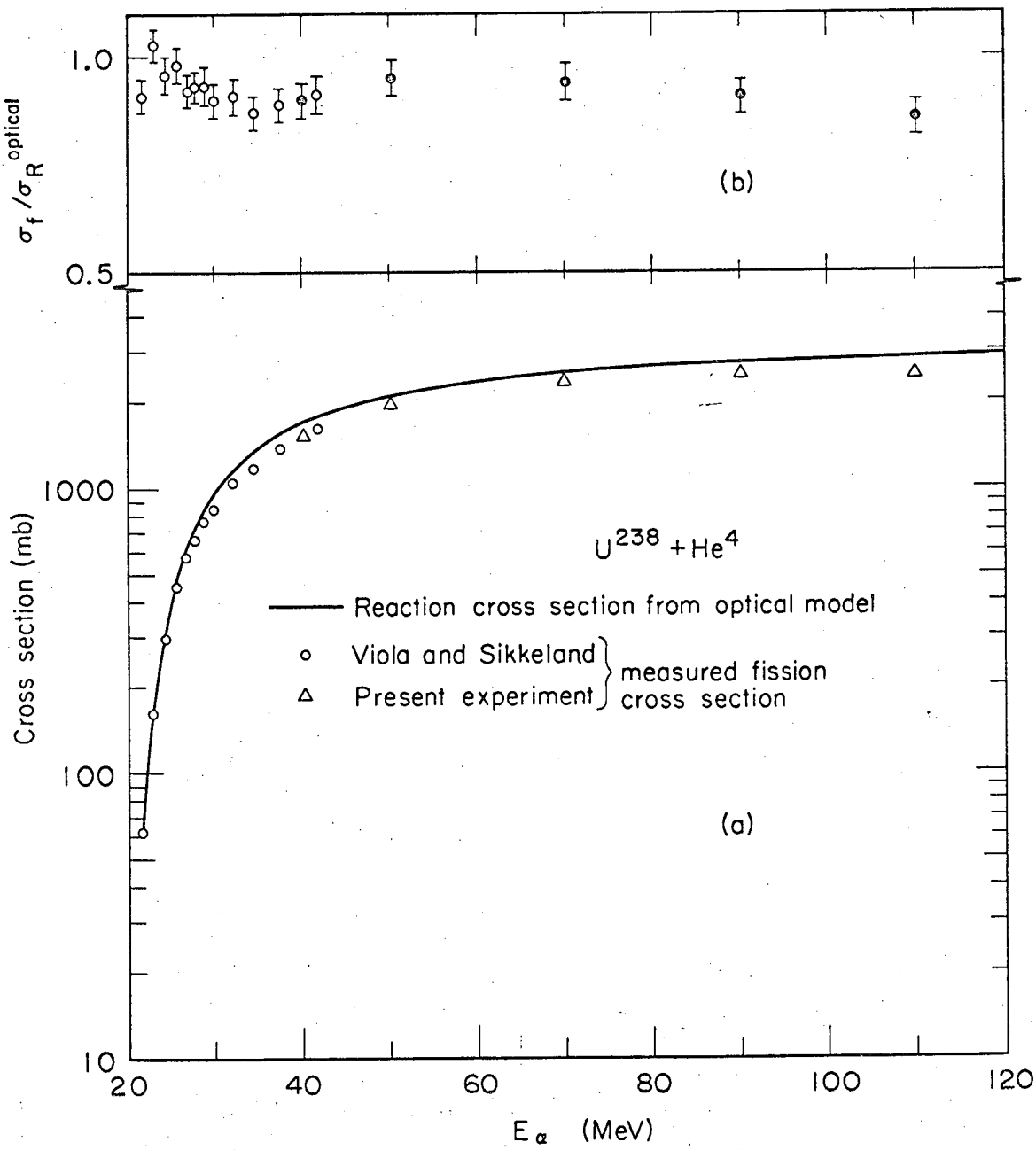

MUB-8962

Fig. 8

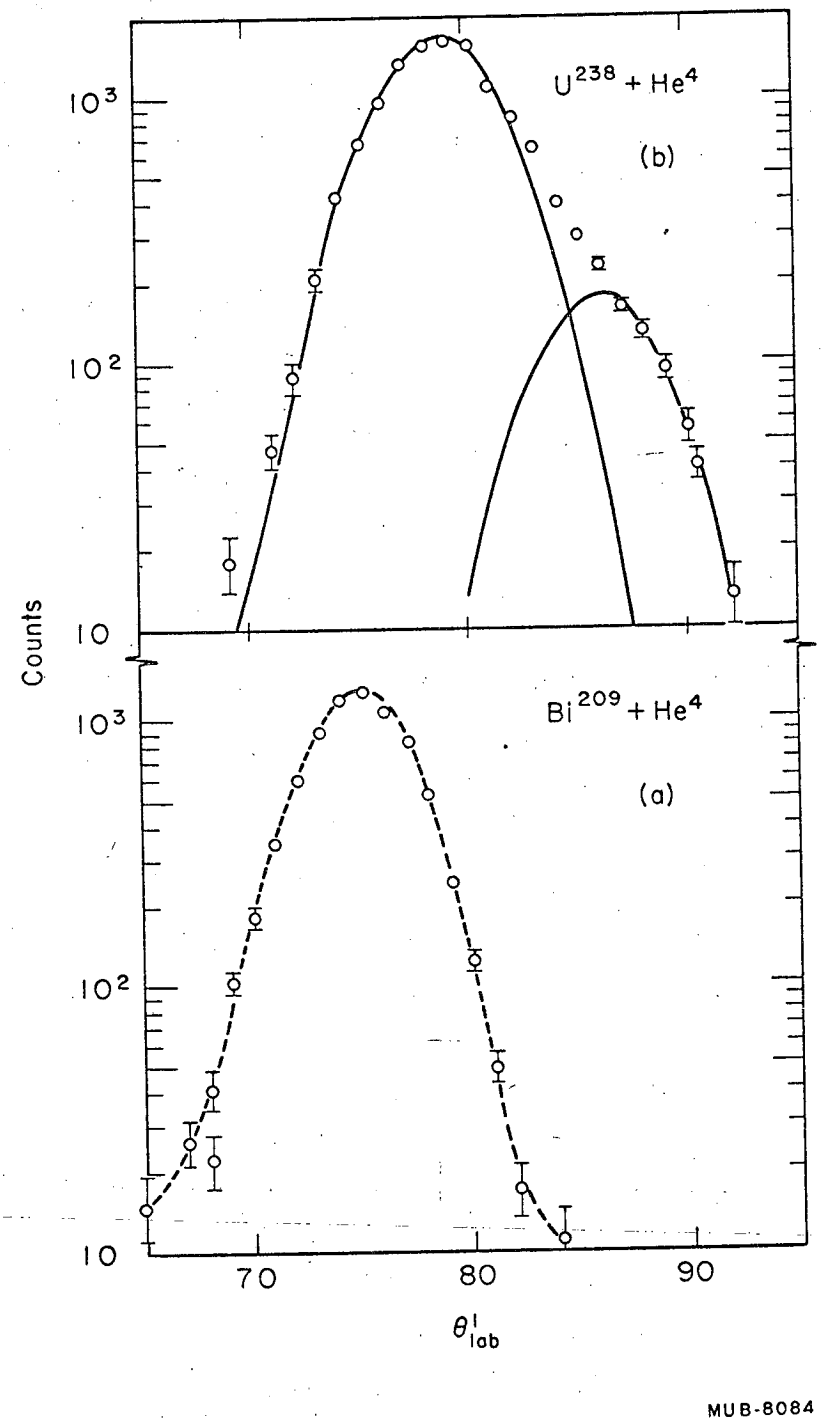

Fig. 9

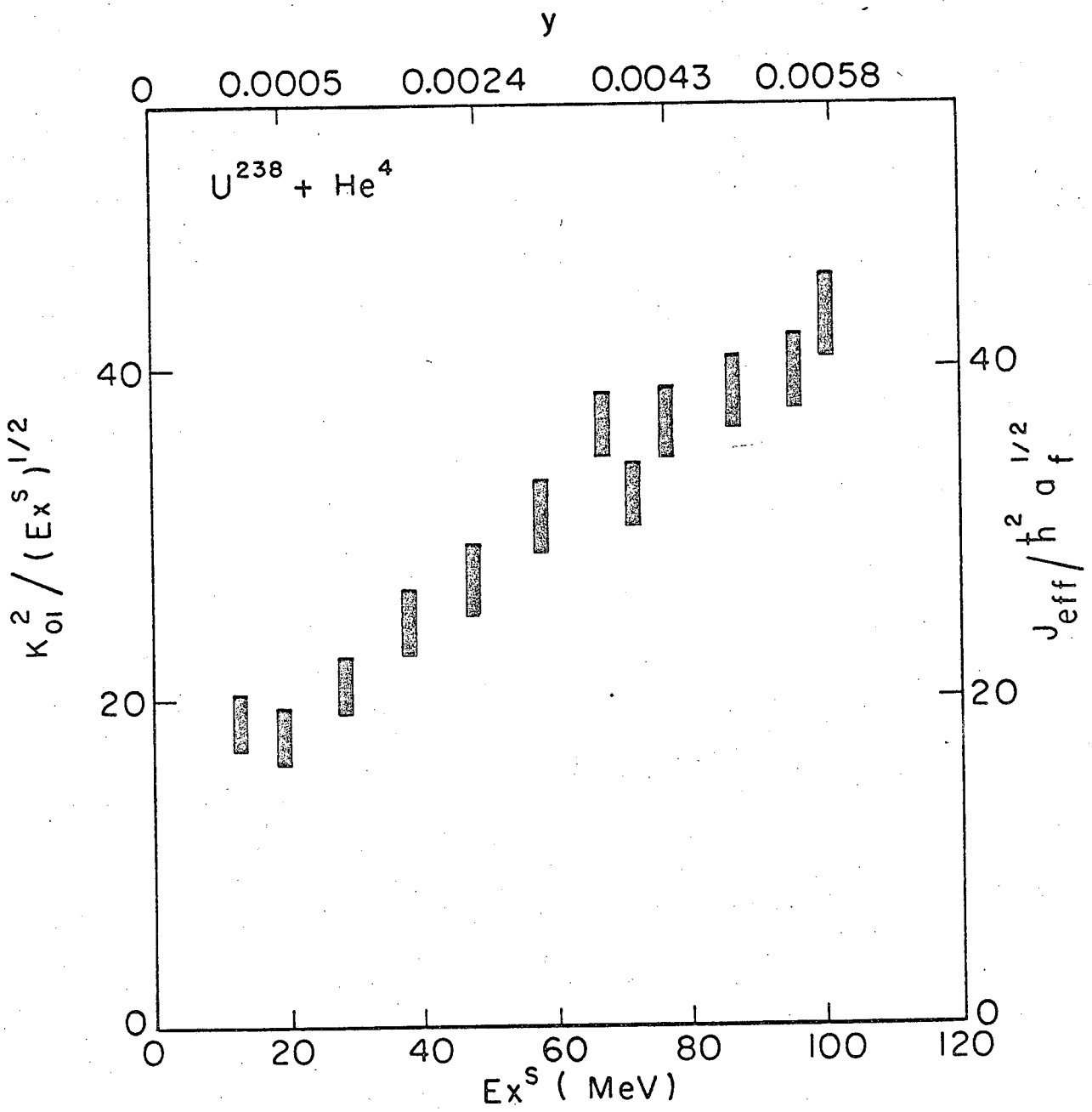

MUB-9486

Fig. 10

This report was prepared as an account of Government sponsored work. Neither the United States, nor the Commission, nor any person acting on behalf of the Commission:

A. Makes any warranty or representation, expressed or implied, with respect to the accuracy, completeness, or usefulness of the information contained in this report, or that the use of any information, apparatus, method, or process disclosed in this report may not infringe privately owned rights; or

B. Assumes any liabilities with respect to the use of, or for damages resulting from the use of any information, apparatus, method, or process disclosed in this report.

As used in the above, "person acting on behalf of the Commission" includes any employee or contractor of the Commission, or employee of such contractor, to the extent that such employee or contractor of the Commission, or employee of such contractor prepares, disseminates, or provides access to, any information pursuant to his employment or contract with the Commission, or his employment with such contractor.